Proceedings of ASME Turbo Expo 2004
Power for Land, Sea, and Air
June 14-17, 2004, Vienna, Austria

GT2004-53014

# A Performance Diagnosis of the 1939 Heinkel He S3B Turbojet.

C Rodgers FASME rodgersc@4dcomm.com

## ABSTRACT.

The historical development of the world's first pure jet propelled aircraft, the Heinkel He 178, and its turbojet the He S3B has been extensively documented, however only limited descriptions of the engine and component aero-thermo-dynamic performances have, as yet, been published in open English literature.
The basic He S3B engine flowpath configuration of a radial compressor mounted back-to-back with a radial inflow turbine, intrigued the author as one excellent example of the pre WW11 radial turbomachinery ingenuity and expertise, to the extent that it prompted this diagnosis.
Recognizing that some of the historically quoted HeS3B performance data may be dubious, attempts have been made to coalesce data from multiple sources into a more consistent account by conducting a detailed engine performance analysis.
HeS3B engine performance characteristics are re-created based upon predicted meanline component maps derived from engine drawings and supporting data recently published by AIAA in his biography "Dr Hans von Ohain -Excellence in Flight".
Predicted engine performance parameters at both a five minute and maximum continuous rating are itemized, together with thrust/rpm/temperature variations at part speed conditions.

## NOMENCLATURE.

| | |
|---|---|
| CFS | Volume Flow |
| D | Diameter |
| g | Gravity |
| H | Head |
| JPT | Jet pipe temperature |
| Mn | Mach number |
| N | Rotational Speed rpm |
| Ns | Specific Speed $=\omega\, CFS^{0.5}/(gHad)^{0.75}$ |
| q | Work factor $= \Delta H/ U^2$ |
| RMS | Root mean square |
| RWT | Turbine Normalized Inlet Flow Parameter $= (Wt\sqrt{T_i}/A_n P_i)/ (Wt\sqrt{T_i}/A_n P_i)crit$ |
| SFC | Specific fuel Consumption |
| T | Temperature |
| TIT | Turbine Inlet Temperature |
| U | Tip Speed |
| V0 | Turbine Spouting Velocity $= \sqrt{2g\, Had}$ |
| Va | Turbine exit axial velocity |
| W | Airflow, or relative velocity |
| $\Delta$ | Difference |
| $\eta$ | Efficiency |
| $\omega$ | Angular Velocity |

Subscripts

| | |
|---|---|
| ad | Adiabatic |
| c | Compressor |
| d | Diffuser |
| crit | Sonic conditions |
| i | Inlet |
| n | Nozzle |
| s | Static |
| t | Turbine, or total |

Note all angles relative to the axial plane

## HISTORICAL REVIEW.

The development of the Heinkel He S[1]3B turbojet is extensively documented in Refs 1-8, as the propulsion unit for the world's first pure jet propelled aircraft to fly, the Heinkel Hs 178.
The He S3B turbojet was the culmination of the pioneering efforts of Dr Hans von Ohain, Conner (1), in combination with his primary associates Dipl.-Ing Wilhelm Gundermann, and Max Hahn, all sponsored under the patronage of Dr Ernst Heinkel.
Test demonstration of its predecessor the He S1 hydrogen fuelled turbojet engine in April of 1937 exhibited 130 kpf of thrust at 10000 rpm, thereby solidifying the design principles and combustion technology enough to proceed with an improved engine, the He S3A, for flight testing in 1938 mounted beneath a He 118 dive bomber.

[1] S = Strahltriebwerk = Jet engine

Following several flight tests the He 3A was accidentally destroyed upon landing as a result of fire stemming from a leaking fuel line.
In May 1939 a further improved engine the He S3B was installed in the historic Heinkel He 178 aircraft, but the developed thrust was marginal for aircraft takeoff. The compressor diffuser and turbine nozzle vanes were subsequently modified, which increased thrust sufficiently to qualify the aircraft for first fllght demonstration.

On August 27 1939 the He 178 made its historic six minute flight, piloted by Erich Warsitz who quotes in Conner (1) he "flew at slightly below 600 km/hr". Peter (3), quotes a much lower speed of 400 km/hr.

Major He S3B engine performance at the 5 minute rating[2], privately communicated to the author from E.Prisell (2) are listed below in Table 1.

Table 1. He S3B Major Performance Data.
Sea level 15 C

| | | |
|---|---|---|
| Rating | | 5 minute |
| Pressure ratio | | 2.8 |
| Airflow kg/s | | 12.6 |
| RPM | | 11600 |
| Static Thrust | kgf | 500 |
| TIT | C | 697 |
| SFC | kg/kgf.hr | 1.6 |

In researching the historic records the author uncovered several errors in reported data and cross sections, including the rotational speed, exterior diameter, blade numbers, airflow, pressures, compressor scroll configuration. These errors have hopefully been corrected in this paper as a result of the detailed performance diagnosis presented herein.
A prime ambiguity example appears to be the rotational speed, frequently published as 13000rpm but specifically quoted by Dr von Ohain in Conner (1) as 11600rpm. A probable explanation for this ambiguity is discussed later.

[2] kurzfristig ung 5 min = limit time 5 minutes

## ENGINE FLOWPATH DESCRIPTION .

The He S3B flowpath is shown schematically on Fig 1, which is a composite of both the data from Conner (1) and Koos (6). An annular inlet injested air into a 14 bladed stator-less inducer stage. The inducer functioned basically to generate prewhirl affront of a 16 bladed radial impeller, in addition to providing a slight pressure rise. The individual radial impeller blades were made of duralumin, retained in a steel hub, and attached to the back disc with rivet stems. The impeller blades were slightly curved at the entry by sheet metal forming of the leading edge, to ostensibly match the prewhirl angle from the separate inducer rotor.
Discharge air from the impeller entered a small diameter ratio radial vaneless space, followed by a sheet metal 37 vane radial diffuser with its exit surrounded by a circular standoff collar. This collar had a splitter, which appeared to divert most of the flow axially forward, whilst directing the residual flow aft to serve as combustor dilution air and inner liner wall cooling. The forward flow was turned aft 180 degrees, via 16 peripheral semi-circular chutes which discharged the flow across fuel vaporizer grids at the entry to the primary zone of the annular combustor. A fraction of the forward flow was also used to provide outer liner cooling.

Fuel was first routed from an electric driven fuel pump to the aft turbine bearing housing to provide cooling, and then metered to four circumferentially spaced fuel lines which fed sixteen vaporizer spray bars at the annular combustor entry.
The combustion products discharged from the combustor into the annular bend and accelerated into the 27vane radial turbine nozzle, subsequently impinging upon the 12 bladed turbine rotor. The blade shape of the turbine exducer was formed in similar fashion to the impeller blades by bending over the tip sections. This rudimentary method of blade forming was presumably constrained by expediency, and manufacturing limitations. The turbine blades were also rivet attached to disc backplate. A photograph of the He S3B replica in the Deutsches Museum Munich is shown on Fig 2.

The rotating assembly was supported by two bearings. A deep grove split inner race ball bearing was located in the central housing between the inducer and impeller, and lubricated with oil from

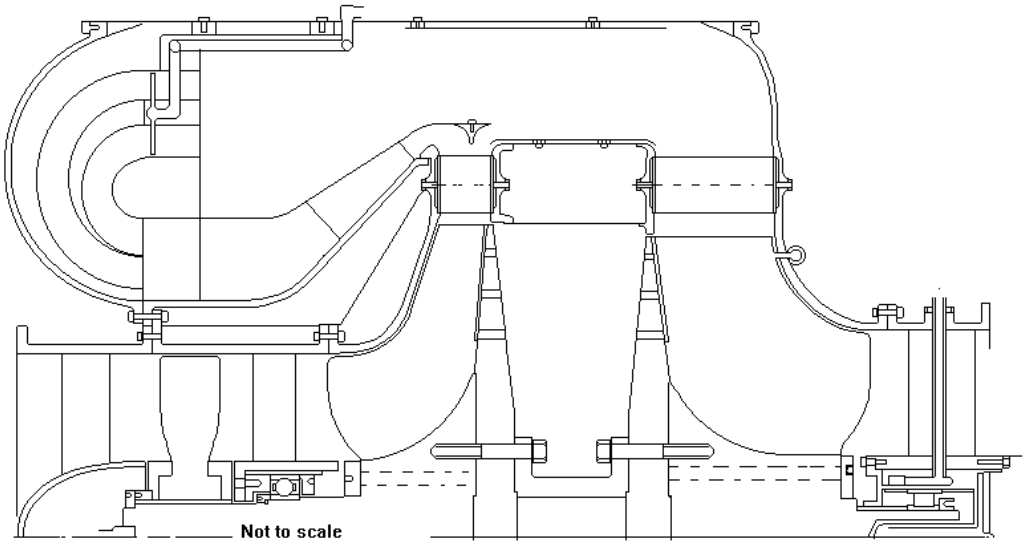


**Fig 1 He S3B Turbojet Cross Section**

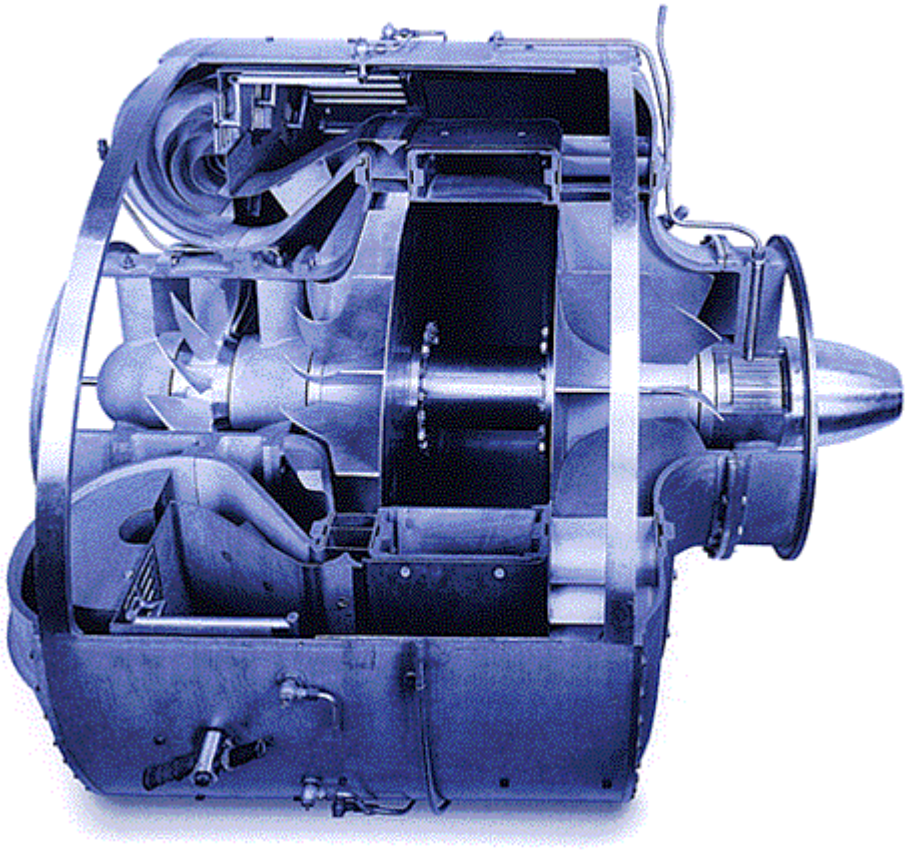

**Fig 2 HeS3B Replica, courtesy Deutsches Museum**

an encapsulated container. The aft roller bearing was of the grease pack type with extra cooling from the fuel supply. There were significant problems adequately lubricating the relatively small bearings as a result of the axial thrust and un-balance loads created by the large diameter compressor and turbine rotors. Apart from continued combustor refinements the second major focus of the development effort was achieving increased flow and higher component efficiencies.
Dr Ohain conceived the key to more efficient operation at higher compressor inlet relative Mach numbers (inherent with increased airflow capacity), was a separate small blade camber axial inducer.

Sir Frank Whittle (4) chose an alternate solution to increase airflow without encountering higher inducer Mach numbers by selecting a double-sided centrifugal impeller. Whittle's solution did however require development of inlet turning vane cascades to improve inlet flow mal-distribution effects.

Engine starting was accomplished with pressurized air fed to impingement nozzle(s) mounted on the turbine housing close to the turbine rotor tip.

## COMPONENT PERFORMANCE PREDICTION.

The analytical procedure utilized to re-create the He S3B turbojet performance comprised patching the historic data with current turbomachinery centrifugal compressor and radial inflow turbine 1D prediction procedures, in an iterative loop. An initial turbojet performance model, matching the Table 1 data was compiled, and successively refined with individual component performances and matching predictions.
One major performance parameter previously absent in the majority of the historic data was the turbine inlet temperature (TIT). The historic data relating to German gas turbine development in WWII focus upon the strategic importance and shortage of high temperature materials suitable for turbine rotor and blade manufacture. Consequently after the historic He 178 flight German gas turbine engineers proved their ingenuity in developing air cooled turbine blades for gas turbine quantity production.

Wagner (5) discloses that Krupp product P193 was used for the He S3B turbine nozzles and rotor blades, with heat resistant cast steel for the rotor hub, with no mention of the operating temperature. It would appear that with these rotor materials the He S 3B turbojet would be limited to a TIT no higher than 700 C (1292 F) matched to the 11600 rpm rated speed by appropriate jet nozzle sizing.
It is remarkable that the fabricated rotor assembly with separate sheet metal blades, attached with De Laval roots in the hubs, and riveted to the back discs, apparently survived operation at the maximum thrust conditions, particularly the turbine. Some industrial centrifugal compressor impellers and fans were still manufactured using this technique as late as the 1950's, but operating at rather lower tip speeds and temperatures. Apparent too is that the He S3B rotor assembly had no intervening heat shield between both rotor discs, which may have caused radiation heat pickup from the hot turbine on to the impeller disc backface.

## PRELIMINARY CYCLE ANALYSIS.

A simple Brayton cycle model of the HeS3B turbojet was first created, assuming constant compressor and turbine gas properties. The relatively large sheet metal casing and flimsy flanges could potentially have been susceptible to leakage between the compressor and turbine, thus an external leakage equal to the fuel flow input plus 1% was assumed, (i.e., $W_t/W_c$=0.99). The model was used to initially assess the compressor and turbine efficiencies that could have satisfied the overall performance level of Table 1, using TIT as a parameter. Cycle results are shown on Fig 3 indicate that if the TIT was no higher than 700C the approximate adiabatic compressor and turbine efficiencies were plausibly of the order 73% and 83% respectively.

## COMPRESSOR PERFORMANCE PREDICTION.

The major compressor geometric features as determined from the Ohain drawings are shown on Fig 4, and depict the small inducer hub diameter and relatively short axial chord of the impeller. The 14 separate inducer blades were forged from duralumin and stacked on a stub shaft extending from the main shaft. Contour milling a combined inducer and impeller from a single billet could have been manufactured, but the time and expense was probably prohibitive. For example prototype mixed flow impellers of the He S 011 developed in 1942 were reported to have required some 3000 hrs!, Kay (7), to machine from a single billet. No wonder a manufacturing change was implemented later to a HeS3B inducer type fabricated assembly with individual forged blades.

The simple channel diffuser with a vane number of 37, and diameter ratio of 1.2 is shown on Fig 4. As mentioned previously the diffuser discharged against

a circular standoff collar, which split the flow both forward, and partly aft.
The forward flow traversed through a second diagonal deswirl cascade before entering the semi circular turning chutes.

The compressor geometric features combined with the preliminary cycle analysis compressor efficiency (total-static) prediction of 73% were used to derive the plausible 1D "design point" compressor performance parameters listed in table 2.

Table 2. Compressor Performance Parameters.

| | | |
|---|---|---|
| Airflow | kg/s | 12.6 |
| Pressure ratio | t-s | 2.8 |
| Rotational speed | krpm | 11.6 |
| Stage efficiency | % (t-s) | 73 |
| Specific speed | Nsc | 0.69 |
| Inducer tip diameter | mm | 380 |
| Inducer hub diameter | mm | 158 |
| Inducer blade number | | 14 |
| Inducer RMS blade angle | | 45 |
| Inducer tip rel Mn | | 0.70 |
| Inducer throat area | $cm^2$ | 590 |
| Impeller tip dia | mm | 640 |
| Impeller backsweep | deg | 0 |
| Impeller tip width | mm | 54 |
| Impeller tip gap/blade | % | 5 |
| Impeller work factor q | | 0.906 |
| Impeller blade No | | 16 |
| Impeller tip Mn | | 0.90 |
| Impeller diffusion $W_1/W_2$ | | 2.3 |
| Diffuser Vane No | | 37 |
| Diffuser throat area | $cm^2$ | 245 |
| Diffuser area ratio(exit/throat) | | 2.2 |
| Diffuser recovery | | 0.63 |
| Impeller + inducer $\eta$ | % | 88.0 |

The compressor specific speed, Nsc, was close to optimum, and the inducer tip entry relative Mach number moderately high by pre WW II standards. This combination of Nsc and Mach number would have placed the radial bladed impeller type design near the maximum attainable efficiency levels for 1939 centrifugal compressor design state-of-art.

The derived compressor work factor q =$\Delta H/ U^2$ is 0.906; indirectly verifying the rotational speed was 11.6 krpm. Had the speed been 13 krpm the impeller work factor would have reduced to 0.72, more typical of an impeller with the blades sweptback at some 40 degrees.

The engine frontal area limitations in the He 178 aircraft confined the radial extent of the vaned diffuser, which coupled with the flowpath contortions from the circumferential exit collar, diagonal deswirl cascade, and 180 deg chutes probably precipitated reduced overall static pressure recovery. The radial diffuser high vane count was assessed to produce good covered channel recovery, but with full loss of the exit dynamic head the predicted overall diffuser static pressure recovery was 0.63, loitering the overall stage total–static efficiency at the 73% level.
The comparatively large impeller tip width is thought to have over-loaded the impeller relative velocity diffusion ratio $W_1/W_2$, such that compressor surge margin may have been limited.

Upon formulation of this initial compressor "design point" analysis the next step was to predict the credible compressor performance map Rodgers (9) shown on Fig 5, portraying corrected inlet flow vs stage pressure ratio, with corrected speed parameters of 100, 90, and 80. Superimposed on Fig 5 is the estimated engine operating line (to be discussed later) that indicates a comfortable compressor surge margin of some 20% at 100% speed.
It is strange that no mention of encountering compressor surge problems appears in the quoted references, perhaps this could have been further justification why Ohain selected a simple centrifugal compressor. His major justification was in fact, that although he recognized the merits of axial compressors for higher thrust/frontal area, he did not have access to compressor test rigs suitable for testing and matching of numerous axial flow compressor stages.

COMBUSTOR PERFORMANCE.
Dr von Ohain realized upon embarking of his endeavors that the key to obtaining reliable, efficient combustion with consistent starting characteristics was vaporization of liquid fuel.

The HeS1 hydrogen engine had already been demonstrated, and with this to his credit his next inspiration was vaporization of liquid fuel.

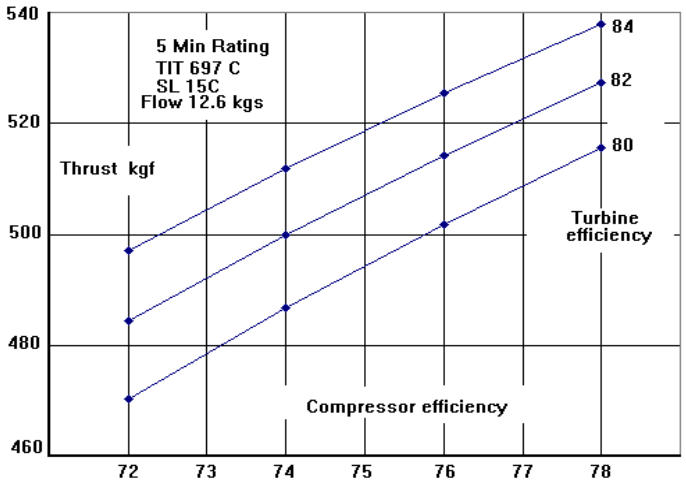


**Fig 3. Compressor and Turbine efficiencies**

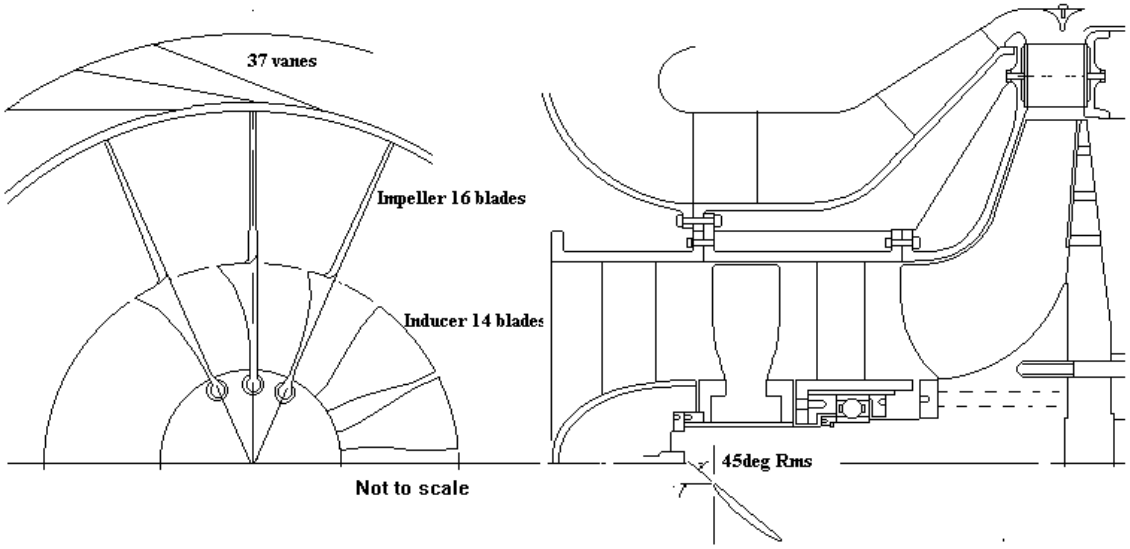


**Fig 4. Compressor Design Features**

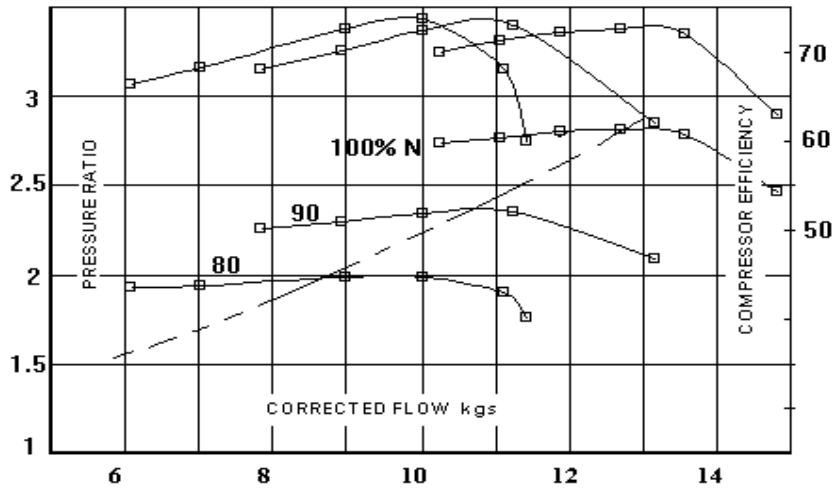


**Fig 5. Derived Compressor Map**

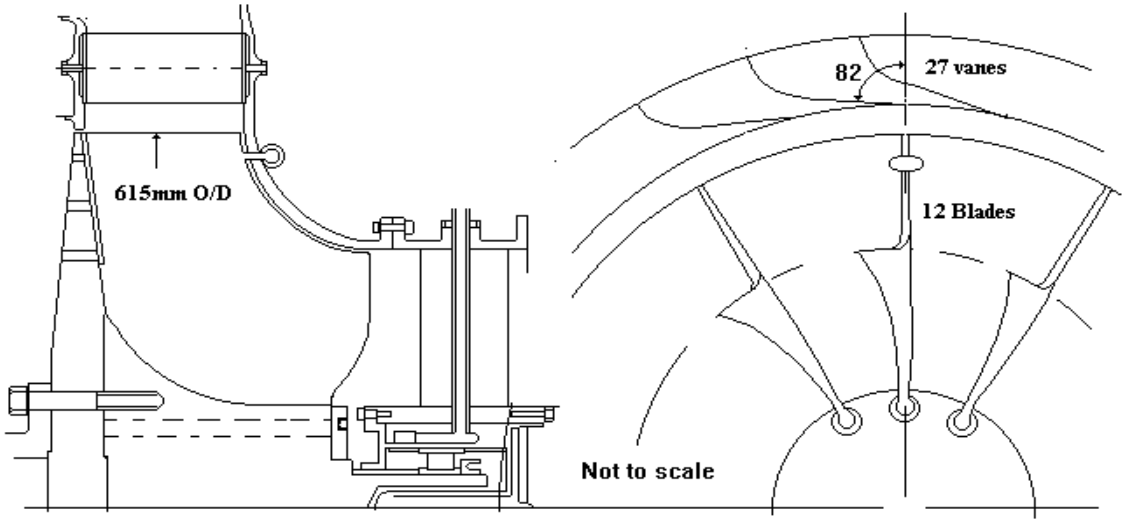


**Fig 6. Radial Inflow Turbine Design Features**

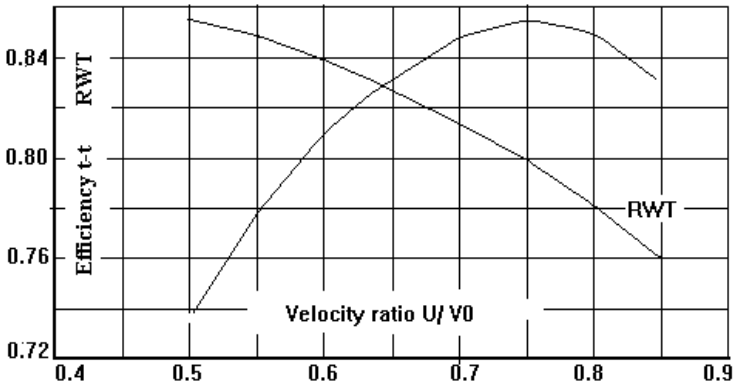


**Fig 7. Derived Turbine Performance**

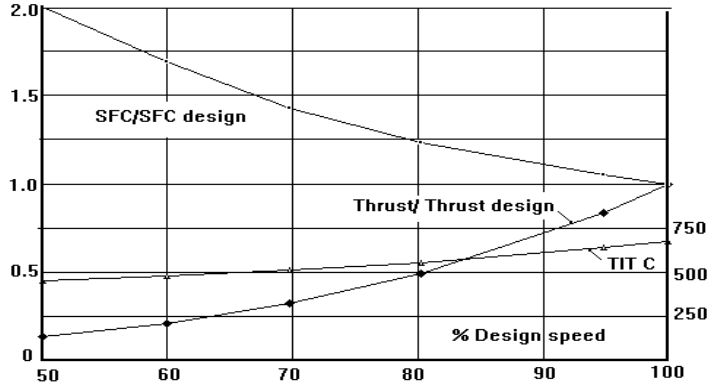


**Fig 8. Turbojet Part Load Performance**

This he cleverly surmounted by initiating combustion with hydrogen, which heated the vaporizer spray grid bars to a temperature sufficient to then enable switching over and vaporizing gasoline. Combustor temperature distribution patterns however still often caused localized carbon deposits on the spray bars.
The liquid fuel was first routed to assist cooling of the aft bearing housing, and then routed to the spray bar array depicted on Fig 2 which served for fuel vapor injection and to aid fuel/air mixing by means of turbulence.

One characteristic of vaporizer type fuel injectors is decreasing combustion efficiency with decreasing thrust, with the possibility of blow out below idle thrust conditions yet von Ohain notes Ref 1 "the combustor had a wide operational range which made it possible to start the engine easily and fly at different speeds and altitudes with an accelerating or decelerating engine". Additionally Ohain commented that the combustor was designed for low pressure drop without specifying the magnitude. The author estimated a pressure drop of the order 4%, from the compressor diagonal deswirl cascade exit to the turbine nozzle vane leading edge. Prisell (2) mentions a higher loss of 7%, which may have been from the radial diffuser exit to turbine nozzle.

The largest discrepancy in the combustor data is however the difference between the commonly published SFC's of 1.6, and that derived herein of 1.45 kg/lbf.hr, is addressed later.

## TURBINE PERFORMANCE PREDICTION

The HeS3B radial inflow turbine geometric features as defined by Conner (1) drawings are shown on Fig 6, and illustrate the exceptionally wide, short radial chord nozzle, and matching rotor entry wide blade height. The design logic is reported to have increased the turbine blade height in proportion to the compressor blade height and gas density change, but engine frontal area concerns appear to have also limited the radial extent of the turbine nozzle. As a consequence low entry radial velocity would require increasing nozzle deflection and higher rotor incidence changes.
The sheet metal turbine nozzle vanes were formed to provide the required exit throat area, with presumably zero inlet incidence. As such the thin nozzle leading edge could have been sensitive to residual combustor exit swirl discharging from the combustor inner liner. The derived turbine nozzle throat area of 438 $cm^2$ listed in table 3 was used to calculate a vane trailing edge angle of 83.4 degrees as compared 82 degrees depicted on the turbine drawing Fig 7. This is surprisingly close, especially since Conner (1) reports "the design team made several refinements to the easily exchangeable radial cascades of the compressor diffuser and turbine stator".

The exducer portion of the turbine rotor was simply formed by benching over the tip trailing edges against a pre-formed die. Examination of Fig 2 shows that the trailing edge bending was small at the tip and (by construction)) zero at the hub, thereby under-turning the flow, with high exit swirl in the direction of rotation.

Table 3. Turbine Performance Parameters.

| | | |
|---|---|---|
| Airflow | kg/s | 12.6 |
| Pressure ratio | t-s | 2.0 |
| Rotor blade number | | 12 |
| Rotational speed | krpm | 11.6 |
| Velocity ratio | Ut/ V0 | 0.63 |
| Specific speed | Nst | 0.66 |
| Nozzle Vane No | | 27 |
| Nozzle throat area | $cm^2$ | 434 |
| Rotor tip diameter | mm | 613 |
| Rotor blade number | | 12 |
| Rotor tip speed | Ut | 1225 |
| Rotor tip Mn | | 0.64 |
| Rotor tip width | mm | 122 |
| Rotor tip gap/blade width | % | 5 |
| Exducer | Va/Ut | 0.49 |
| Exducer tip diameter | mm | 418 |
| Exducer hub diameter | mm | 160 |
| Exducer RMS blade angle | | 30 deg |
| Exducer throat area | $cm^2$ | 1017 |
| Exducer RMS exit swirl | deg | -24 |
| Turbine efficiency t-t | % | 83.1 |
| Turbine efficiency t-s | % | 74.7 |

The radial turbine performance prediction codes developed by Rodgers (10), indicated that the He S3B turbine total-total efficiency (t-t) may have been as low as 83.1%, with a total-static efficiency as low as 74.7 %. The low static efficiency is a result of the small exducer annulus area in combination with the higher airflow necessary to attain adequate He 178 thrust margin.
Examination of the estimated turbine performance map shown on Fig 7 indicates a predicted peak total-total efficiency of 85.2% occurring at a U/V0 of 0.7. Had the turbine rotor tip diameter been larger therefore the turbine total-total efficiency may have been increased 2% points.

## JETPIPE NOZZLE.

During the preliminary design of the He 178 Dr von Ohain commented upon the adversely long air inlet and jetpipe, suggesting an alternate design with two engine pods under-slung beneath the wings. Due to the contracted time schedule Dr Heinkel nevertheless insisted on the single engine installation, buried amidships within the fuselage.
Comparative engine installed thrust and static bench thrust calibrations subsequently revealed the longer jetpipe had apparently reduced the effective nozzle throat area causing and alteration in engine matching, thereby increasing TIT vs speed.
The jetpipe nozzle area was therefore enlarged some 7%, which reduced the installed static thrust loss from 15% to less than 7%.
The derived HeS3B turbojet performance model to be discussed later was used to analytically ascertain the effects of a 7% reduction in jetpipe nozzle throat area, and indeed confirmed that a thrust loss of 15% at rated TIT could have occurred.
Additionally note that the predicted exducer RMS exit swirl in table 2 was 24 degrees and may also contribute a reduction in jetpipe discharge coefficient.

No specific data regarding the important jetpipe dimensions and interface with the He S3B exhaust flange could be uncovered. Scaling of the He 178 aircraft drawing from Wagner (5) indicated that the jetpipe diameter was of the order 650 $cm^2$. This is unfortunate has the actual dimensions would have served as another cycle performance balance. It is peculiar that none of the references comment on the final nozzle shape of the He 178 aircraft, which from several photographs externally appears to be oval. Additional correspondence with Prisell (2) stated that the nozzle was more or less rectangular with rounded corners and adjustable flaps, so different nozzle areas could be tested to optimize installed engine performance

## PARASITIC LOSSES.

The parasitic losses may have been relatively small with only two undersized bearings and fuel pump. Although Wagner (5), Koos (6) and Kay (7) show He S3B cross sections with a forward mounted fuel pump. Wagner (5) reports that this was not ready for the inaugural flight of the He 178 aircraft. Two fuel pumps were therefore powered by a small electro-motor fed by an on-board battery.
The occurrence of turbine tip hot flow leakage to the compressor tip appears to have been possible as drawings show no rotor tip seals, other than close radial gaps.

The compressor and turbine performance predictions herein show the ratio of the turbine rotor tip to the compressor rotor tip pressure at rated thrust could have been fortuitously equal, but the probability of flow leakage did most likely occur at some turbojet operating condition.
Tip leakage either into the compressor or turbine, for back-to-back rotor assemblies, is known by the author to reduce component efficiencies.

## COMPRESSOR AND TURBINE MATCHING.

The three critical single shaft turbojet geometric parameters are;
1). The final jetpipe nozzle area.
2). The compressor diffuser throat area.
3). The turbine nozzle throat area.

The jetpipe nozzle area essentially establishes the relationship between speed versus TIT and the position of the operating line on the compressor map, besides indicative of the flow function $W\sqrt{T}/P$ at the nozzle entry. The compressor diffuser throat area primarily governs the compressor surge and choke margins, and the turbine nozzle area influences both compressor match point and speed versus TIT, albeit the latter to a lesser degree than the jetpipe area. The compressor diffuser and turbine nozzle throat areas also reflect the flow function at the impeller exit and turbine nozzle inlet, thus all three areas provide important correlating factors in re-creating both the engine and component performances.

It had been hoped to compare the three throat dimensions calculated from both engine and component performance estimates with those from Conner (1) drawings, but unfortunately the drawing data is inadequate. Drawing scaling comparisons did however show the throat dimensions were of the same order of magnitude as the analytical computations.

## TURBOJET PERFORMANCE ANALYSIS.

As discussed previously the analytical procedure utilized to re-create this performance model comprised patching the historic data with current turbomachinery centrifugal compressor and radial inflow turbine 1D prediction procedures, in an iterative loop. The finalized predicted turbojet performances at both the 5minuute and maximum continuous ratings are listed in table 4.

**Table 4. Predicted He S3B Turbojet Performance Uninstalled Sea Level 15 C.**

| Rating | | 5 min | max cont |
|---|---|---|---|
| Rotational speed | krpm | 11.6 | 11.2 |
| Pressure ratio | | 2.84 | 2.71 |
| Compressor efficiency | % | 73.4 | 73.4 |
| Diffuser throat area | $cm^2$ | 245 | 245 |
| Airflow kg/s | | 12.6 | 12.1 |
| Combustor loss % | | 4 | 4 |
| Combustor efficiency | % | 90 | 90 |
| Turbine efficiency | % | 83 | 83 |
| Nozzle throat area | $cm^2$ | 438 | 438 |
| Flow ratio Wt/Wc | | 0.99 | 0.99 |
| Mechanical efficiency | % | 98 | 98 |
| TIT | C | 697 | 672 |
| JPT | C | 573 | 558 |
| Jetpipe nozzle area | $cm^2$ | 708 | 708 |
| Jetpipe thrust coefficient | | 0.98 | 0.98 |
| Thrust | kgf | 500 | 450 |
| SFC | kg/kgf.hr | 1.43 | 1.45 |

The derived engine SFC is based upon an assumed combustor efficiency of 90%. This is lower than the 1.6 level of data (1-7), posing the query, was the combustor efficiency possibly lower, at 82%?. If so it could have been evident from a profusion of black exhaust smoke and carbon deposits.
The predicted compressor and turbine maps Figs 5 and 7, were used to compute the He S3B part load performance shown on Fig 8.
At 50 % design speed the estimated thrust was 60kg, compared to Ref 1 documentation of 70 kg.

As previously noted the part load operating airflow vs pressure ratio characteristic is shown super-imposed on the compressor map Fig 5.

## He S6 TURBOJET.

During 1939 a higher performance version of the HeS3B was developed. Speed was increased to 13.3 krpm, with thrust increasing to 550 kgf. The engine outside diameter (O/D) may also have been slightly reduced to 930 mm, Kay (Ref 7). This O/D also coincides with Heinkel archive engine cross section drawing, Fig 9, from Koos and Carter Ref (6 and 11), and differs in several respects from the cross section charted by Von Ohain.
Although archive cross section is dated July 1938, it appears highly probable that this may have been the He S6. The most immediate modification to the He S3B, would have been reduced rotor tip diameter to produce the same pressure ratio at the higher speed and airflow, without major increases in rotor blade stresses. This would account for the larger rotor radial vaneless spaces depicted on Fig 9.

This is however speculative and unconfirmed so that the He S6 data therefore unfortunately adds to the dilemma of trying to confirm the exact configuration of the HeS3B.

## CONCLUSIONS.

Recognizing that some of the historically quoted HeS3B performance data may be dubious, attempts have been made to coalesce data from multiple sources into a more consistent account by conducting a detailed engine performance analysis.
It is lamentable that a complete development documentation of the first turbojet to fly was either destroyed, or was restricted by secrecy constraints. Lingering doubts still remain in the validity of many assumptions and supposedly factual reported data contained within this diagnosis.
Even the detailed drawing information published in his biography, Conner (1), was specified by Dr von Ohain to a draughtsman he commissioned in 1974. This was thirty for years after the first flight of the He 178, so that unless original drawing fragments existed he probably had a remarkable memory.
The author had hoped that sufficient geometric data could have been recovered to construct a full He S3B CFD model, and thereby substantiate the 1D performance predictions. Hand forming of the impeller blade leading edges and turbine exducer trailing edges, plus sheet metal construction of both stators could not defined with sufficient accuracy to justify an extensive CFD analysis at this stage.

In contemplation how could the design of the He S3B have been improved at that historic interval in time?. The analysis described in this paper reveals that minor improvements could have been made to the turbomachinery, had not aircraft frontal area concerns been overwhelming. Turbine inlet temperature and rotor stress limits mandated the desired thrust could only be attained by increased airflow, which coupled with the combustor design, sizing, and placement problems, formulated the unique He S3B flowpath.
With more combustor design alchemy in hand, Dr Ohain's first production engine design, the He S8A, shown on Fig 10, doubled the thrust/frontal area.

## ACKNOWLEDGMENT.

Had all the He S3B historic data been more consistent the author would have felt more confident in the findings of this diagnosis, nevertheless he extends his appreciation and thanks to the all referenced authors except Refs (9 and 10), and notably Conner and Prisell Ref (1and 2), without which the paper could not have been conceived and written.

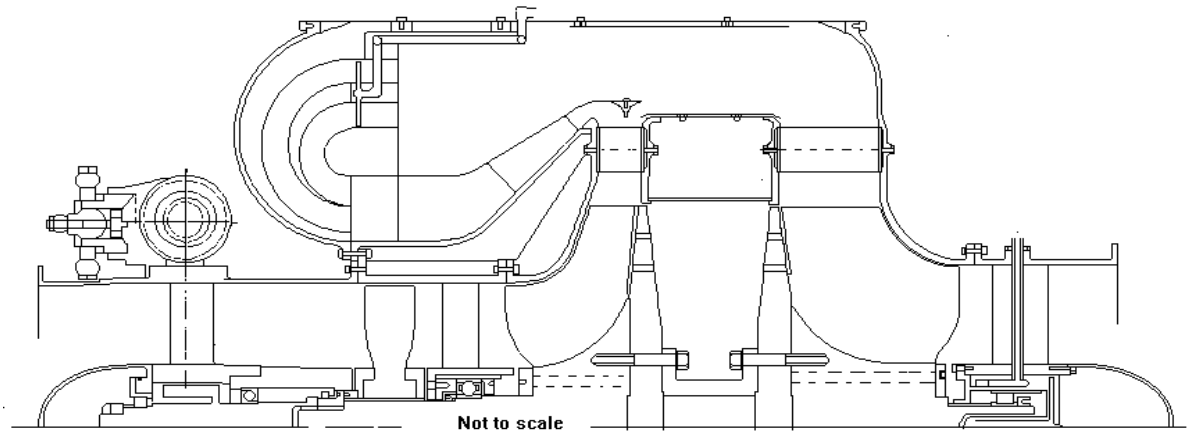


**Fig 9. Probable Heinkel He S6 Cross Section.**

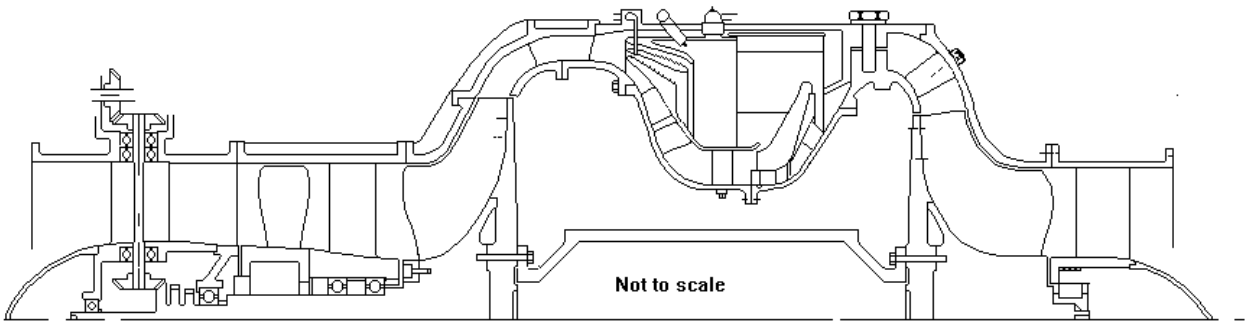


**Fig 10. Heinkel He S8 Cross Section**

**REFERENCES.**

**Ref 1. Conner.M., " Hans von Ohain- Excellence in Flight". AIAA 2002.**

**Ref 2. Prisell. E ., Private communication with author. Aug 5 2003.**

**Ref 3. Peter. J., "The History of Aircraft Gas Turbine Engine Development in the United States" ASME IGTI 1999.**

**Ref 4. Whittle.F., "Gas Turbine Aero-Thermo-Dynamics". Pergamon Press 1981.**

**Ref 5. Wagner.W. " The First Jet Aircraft". Schiffer Military/Aviation History. Atlgen, PA. 1998.**

**Ref 6. Koos.V." Die Entwicklung des ersten flugfahigen Strahltriebwerkes der Welt bei den Ernst Heinkel Flugzeugwerken Rostock". Jet & Prop Jan 2002.**

**Ref 7. Kay. A.L. "German Jet Engine and Gas Turbine Development 1930-1945". Airlife England . 2002.**

**Ref 8. Meher-Homji. C.B., Prisell.E., "Pioneering Turbojet Developments of Dr Hans Von Ohain- From the He S1 to the He S011". ASME JEP April 2000, Vol 121.**

**Ref 9. Rodgers. C. "Performance Characteristics of Radial Compressors". ASME GT-14 1963.**

**Ref 10. Rodgers. C. "The Characteristics of Radial Turbines for Small Gas Turbines".ASME 38026. 2003.**

**Ref 11. Carter.J.l. "Ernst Heinkel Jet Engines" US Navy BUAER Translation May 1945.**

 